

Green River basin 3-D/3-C case study for fracture characterization: Analysis of PS-wave birefringence

James Gaiser* and Richard Van Dok, *WesternGeco*

Summary

An important application of 3-D converted P to S-waves (PS-waves) is to exploit S-wave birefringence (splitting) for delineating reservoir fractures. In azimuthally anisotropic media, fracture intensities and orientations are directly related to traveltimes differences between the fast and slow S-wave and the polarization direction of the fast S-wave, respectively. A 3-D data set from the Green River basin, Wyoming has had common-azimuth processing to optimally preserve the azimuthal effects of S-wave splitting. Analysis techniques to help characterize a fracture setting are demonstrated using this data. Ratios of fast (PS_1) and slow (PS_2) average velocity are particularly important to identify the vertical extent of overburden anisotropy, as well as reservoir horizons. Overburden effects can be removed by 2Cx2C Alford rotation and layer-stripping analyses before characterizing deeper horizons. In addition, less quantitative attributes, which are very sensitive indicators of S-wave splitting, can be employed such as residual off-diagonal 2Cx2C amplitudes after overburden removal and isochron differences between PS_1 and PS_2 . Combining these attributes with traditional structural and stratigraphic information should provide a more complete geologic interpretation and insights into potential reservoirs with fracture porosity.

Introduction

Converted waves are potentially very useful for fracture characterization because they enable exploiting the effects of birefringence on the upgoing shear waves (S-waves). Ata and Michelena (1995) acquired three 2-D lines centered on a well. Although the spatial coverage was sparse, azimuthal anisotropy appeared to be caused by two fracture systems. A small 3-D/3-C survey collected in the Wind River basin in Wyoming, to calibrate a larger P-wave effort, had some measure of success in characterizing fracture anisotropy (Gaiser, 1999; and Grimm et al., 1999). However, data quality was poor and azimuths were limited. In 2000, the first marine 3-D/3-C survey was acquired at the Emilio field in the Adriatic for the purpose of characterizing fracture porosity (Gaiser et al., 2001).

The objective of this study was to characterize fracture anisotropy in Cretaceous sandstone reservoirs located at depths between 3000 and 4500 m in the Green River basin using a 3-D/3-C survey. Care was taken in the survey design phase to insure good azimuth and offset coverage by having 14 live-receiver lines per swath spaced 536 m apart.

A brick shot pattern was acquired to yield an average fold of 24 over 50 km². The entire survey was oriented NS/EW.

In this paper, three analysis techniques are presented which take advantage of the wide azimuth data to provide important attributes for characterizing fractures. Prior to analyzing PS-wave birefringence, common-azimuth processing of the 3-D data was conducted. PS_1 and PS_2 directions were identified and used to optimally preserve the azimuthal effects of S-wave splitting (Van Dok et al., 2001). Also, 2Cx2C Alford (1986) rotation adapted for PS-waves (Gaiser, 1999) provided a means to combine the multi-azimuth data into a single 2Cx2C volume (the 4-components: PS_{11} , PS_{12} , PS_{21} , and PS_{22}) after application of azimuth-consistent residual statics.

Overburden Analysis

One of the most important steps in using PS-waves for fracture detection is to quantify the overburden azimuthal anisotropic properties and remove the detrimental effects S-waves suffer. These properties include the orientation of the principal S-wave directions, used to identify fast and slow waves for processing, and the differential velocity between the fast (PS_{11}) and slow (PS_{22}) waves. Using either azimuth supergathers from preprocessing analyses or CDP-migrated data, these properties can be determined from 2Cx2C Alford rotation and Winterstein and Meadows (1991) layer-stripping methods adapted for PS-waves.

Another important property of the overburden is the vertical extent. One approach to estimate the extent of S-wave azimuthal anisotropy in the overburden is to analyze PS_{11} and PS_{22} velocity ratios (Gaiser, 1996) as a function of two-way time. Figure 1 shows an analysis between the fast and slow data located at the well in the northern part of the survey. The vertical axis is PS_{11} two-way time and the horizontal axis is the ratio of $V_{ps_{11}}/V_{ps_{22}}$ average velocity. Variable density represents positive cross-correlation coefficients between the two waves. Depending on the velocity ratio, PS_{22} is stretched (< 1.0) or compressed (> 1.0), and then correlated with the PS_{11} at predefined window times. Contours superimposed on the plot indicate constant time delays of PS_{22} in milliseconds.

A maximum correlation trend can be clearly interpreted and is indicated by the dashed line. This corresponds to the time-variant velocity ratio of $V_{ps_{11}}/V_{ps_{22}}$. Above 1.0 s the trend is unknown. However, below 1.0 s the trend increases to a maximum at about 1.3 s and then roughly follows a 30 ms PS_{22} time delay. In the absence of the upper 1.0 s of

Analysis of PS-wave birefringence

data, the base of the overburden can be interpreted at about 1.5 s. It represents an interval of relatively homogeneous, azimuthally anisotropic material with constant orientation confirmed by azimuth-supergather analyses (Van Dok and Gaiser, 2001). Notice that the trend increases to the 40 ms PS_{22} time delay contour at about 3.0 s, indicating an increase in S-wave birefringence.

Further processing of the overburden involves layer stripping, or removing the azimuthal anisotropic effects imparted on the PS-wave data by this shallow interval. This can be accomplished over a time window from 0.0 to 1.6 s. The resulting fast S-wave direction and slow S-wave time delays of the overburden are smoothed spatially and then applied to the poststack 2Cx2C volumes.

Target Horizon Analysis

After layer stripping the overburden, the data are in position for further analysis to determine principal S-wave directions and percent anisotropy for deeper intervals. Figure 2 shows the 2Cx2C inline section that intersects the well at the vertical white line. PS_{11} and PS_{22} are the principal components and are aligned down to the base of overburden at about 1.6 s. Also, the off-diagonal components (PS_{12} and PS_{21}) have been minimized down to this same event.

One approach to analyze target horizons below the overburden is to interpret residual amplitudes on the off-diagonal components spatially and temporally. These amplitudes result when there are changes in the orientation of the S-wave principal directions such as at 2.5 s in Figure 1. These changes may be too subtle to be quantified by traditional layer-stripping methods or by velocity ratios, but amplitudes are sensitive to these variations in S-wave properties and can give qualitative insights into regions where fracture orientation may have changed. Figure 3 shows example maps of residual amplitude at about 1.9 and 2.5 s (arrows in Figure 2). For example, the shallower display delineates regions where the principal axis directions may differ from the overburden in the interval between about 1.6 and 1.9 s. Likewise, the deeper display shows the cumulative effect between the overburden and 2.5 s. Horizontal white lines in Figure 3 indicate the location of the inline data from Figure 2.

A more quantitative approach is to measure traveltimes between reflections bracketing targets for both the PS_{11} and PS_{22} waves in the volume in Figure 2. By comparing isochron differences between PS_{11} and PS_{22} , a spatial representation of percent anisotropy can be interpreted for lateral variations in fracture intensity. However, the assumption here is that there is little or no change in the orientation of the principal axes, since additional rotations

are not applied to the data before measuring traveltimes. Constant principal-axis directions are observed in azimuth-supergather analyses located at the two wells indicated in Figure 3, suggesting this assumption is valid. However, the residual off-diagonal energy in Figure 2 suggests subtle changes.

The third approach, which is most quantitative, involves further layer stripping below the overburden. It is important to remember that the property we are analyzing for fracture detection is the transmission effect on S-waves: the birefringence orientation and the time separation. Off-diagonal components are minimized further by 2Cx2C Alford rotations to estimate any change in the direction of the principal axes. After minimization, the separated PS_{11} and PS_{22} waves are correlated to measure the PS_{22} delay and then PS_{22} is aligned with PS_{11} . Since rotation has been included, these traveltime differences should be more representative of the degree of S-wave splitting than the isochron analysis.

As stated above, attributes of residual off-diagonal amplitude, fast S-wave direction and slow S-wave delay can be interpreted as lateral variations in fracture orientation and intensity. Such rock property interpretations should not be used alone to plan new drilling targets. However, when combined with other structural and stratigraphic information these attributes may provide valuable insights into a broader geological model and potential reservoirs containing fracture porosity.

Conclusions

$V_{ps_{11}}/V_{ps_{22}}$ velocity ratio analysis is a valuable tool to quantify the vertical extent of S-wave birefringence as a function of time. As this ratio varies in time, it indicates different layers in the subsurface where birefringent properties may have changed. One of the most important of these layers is the overburden, which can be removed effectively by 2Cx2C Alford rotation and layer-stripping analyses, and leads to quantifying the fracture properties at target horizons. Three analysis techniques (residual off-diagonal amplitudes, PS_{11} and PS_{22} traveltime isochrons, and layer stripping) provide a broad range of interpretation tools and attributes that can help identify lateral variations in fracture properties.

References

- Alford, R.M., 1986, Shear data in the presence of azimuthal anisotropy: Dilley, Texas: 56th Ann. Internat. Mtg., Soc. Expl. Geophys., Expanded Abstracts, 476-479.
- Ata, E., and Michelena, R.J., 1995, Mapping distribution of fractures in a reservoir with P-S converted waves: The Leading Edge, **14**, 664-676.

Analysis of PS-wave birefringence

- Gaiser, J.E., 1996, Multicomponent Vp/Vs correlation analysis: *Geophysics*, **61**, 1137-1149.
- Gaiser, J.E., 1999, Applications for vector coordinate systems of 3-D converted-wave data: *The Leading Edge*, **18**, 1290-1300.
- Gaiser, J.E., Loinger, E., Lynn, H., and Vetri, L., 2001, PS wave velocity variations in azimuthally anisotropic media for layer stripping: 63rd EAGE Conf. and Tech. Exhibit., Extended Abstracts.
- Grimm, R.E., Lynn, H.B., Bates, C.R., Phillips, D.R., Simon, K.M., and Beckham, W.E., 1999, Detection and analysis of naturally fractured gas reservoirs: multi-azimuth seismic surveys in the Wind River basin, Wyoming: *Geophysics*, **64**, 1277-1292.
- Van Dok, Richard, Gaiser, James, and Markert, John, 2001, Green River basin 3-D/3-C case study for fracture

- characterization: Common-azimuth processing of PS-wave data: 71st Ann. Internat. Mtg., Soc. Expl. Geophys., Expanded Abstracts.
- Winterstein D.F., and Meadows M.A. 1991, Shear-wave polarizations and subsurface stress directions at Lost Hills Field: *Geophysics*, **56**, 1331-1348.

Acknowledgments

We thank John Markert, Jonathan Fried and John Young at WesternGeco for his help in processing the converted-wave data for this study. Thanks also to EOG Resources, Tom Brown Inc., and Stone Energy for their participation and for providing valuable insights in the nature of the reservoir.

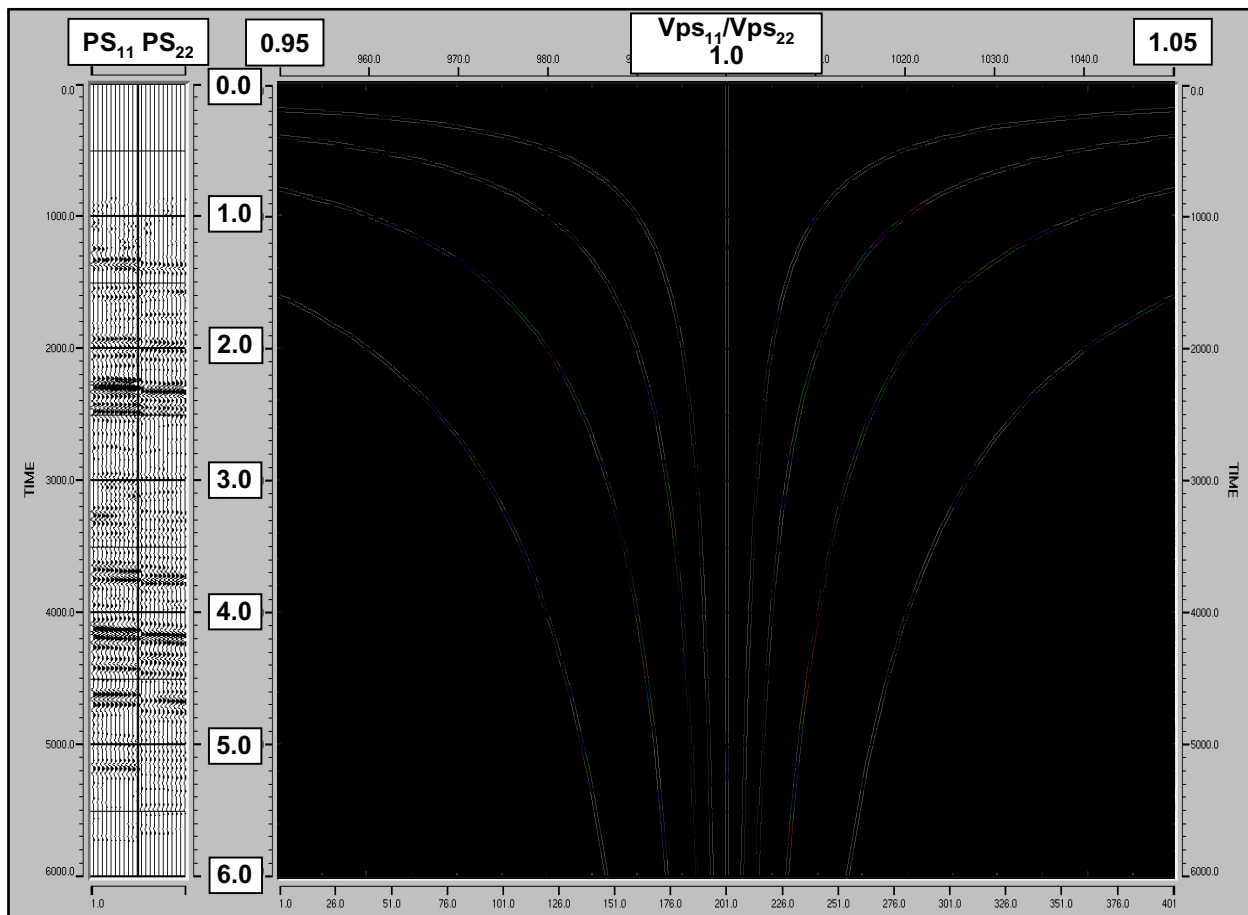


Fig. 1. Average velocity ratio analysis between the PS₁₁ and PS₂₂ traces (left) located near the well in the northern part of the survey. The $V_{ps_{11}}/V_{ps_{22}}$ ratio ranges from 0.95 to 1.05, time is two-way PS₁₁, and variable density represents positive cross-correlation coefficients between PS₁₁ and PS₂₂. Contours indicate constant PS₂₂ time delays and the dashed line shows the interpreted relationship between the split S-waves. The base of the overburden is interpreted at the maximum traveltime difference just below the event at 1.3 s.

Analysis of PS-wave birefringence

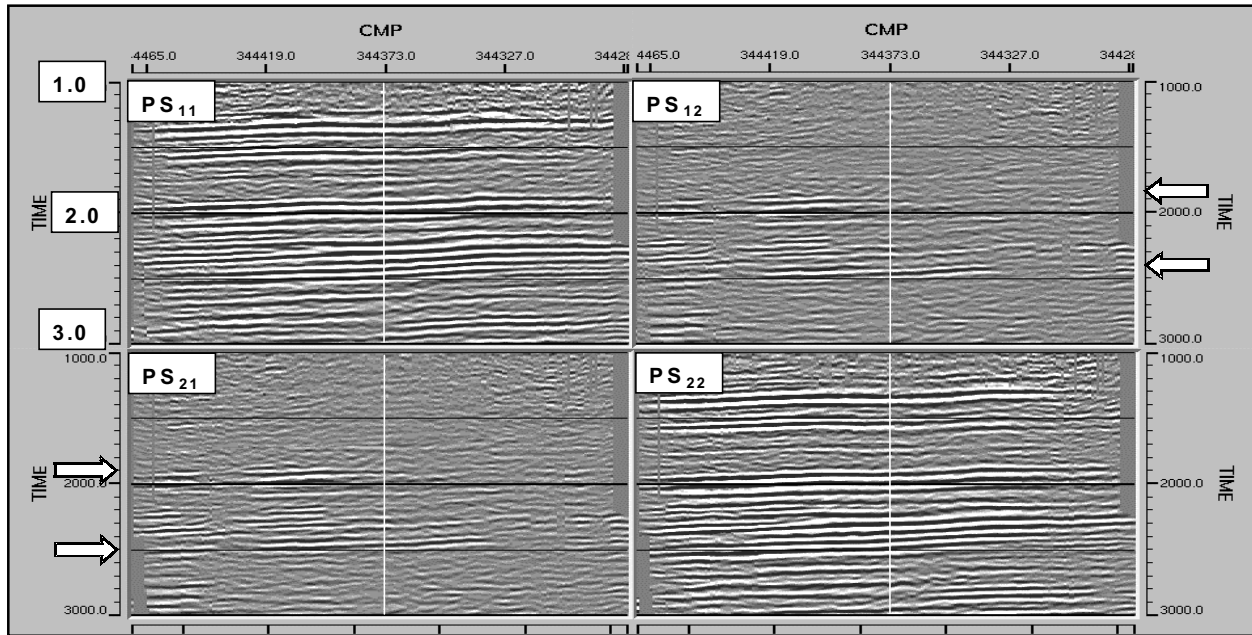


Fig. 2. 2Cx2C inline section after Alford rotation and layer stripping the overburden. PS_{11} and PS_{22} are the principal components aligned through the overburden at about 1.6 s. These components are important for quantitative isochron analyses of percent azimuthal anisotropy. PS_{12} and PS_{21} are the off-diagonal components minimized through the overburden. Residual amplitudes below the overburden on PS_{12} and PS_{21} , shown in Figure 3, provide qualitative insights into changes in principal direction. The vertical white line indicates the location of the well and the $V_{ps_{11}}/V_{ps_{22}}$ average velocity analysis in Figure 1.

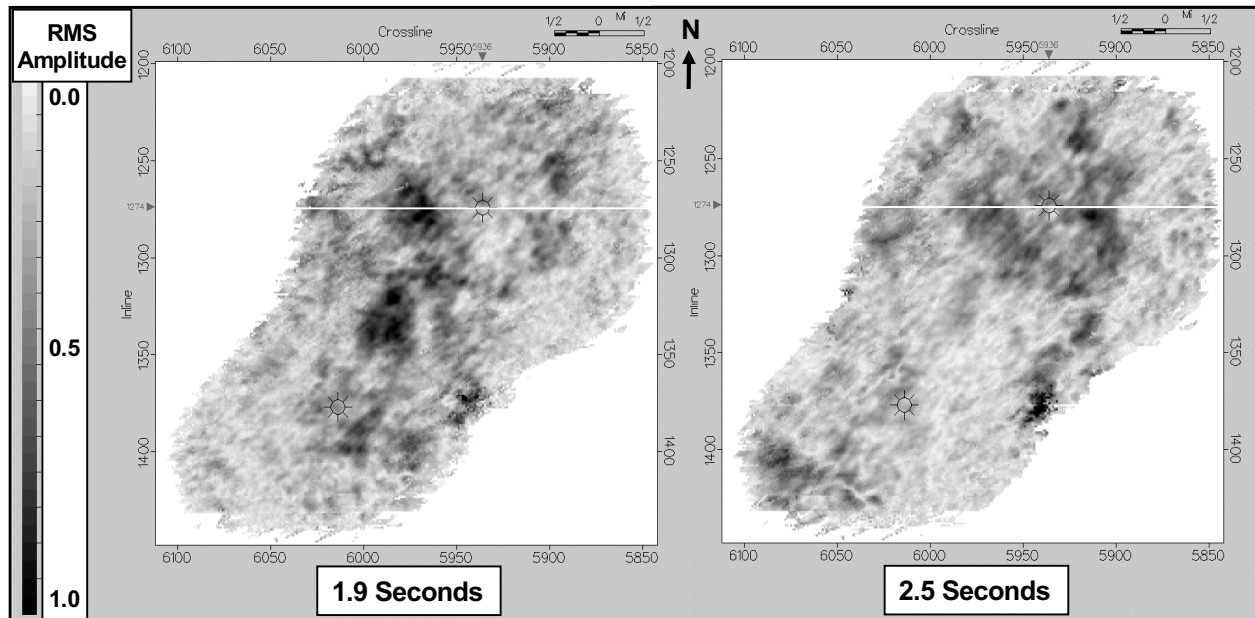


Fig. 3. Attribute maps of residual amplitude from the off-diagonal components in Figure 2 at the two arrows. The horizontal white line shows the location of the 2Cx2C inline section in Figure 2 intersecting the well at the center. High amplitude areas indicate qualitative changes in birefringence where S-wave splitting properties differ from that of the overburden properties. These areas could be related to a change in the orientation of the principal axes.